

# DesignCon 2008

## Validation Methods for S-parameter Measurement Based Models of Differential Transmission Lines

Peter J. Pupalaikis, LeCroy Corporation  
PeterP@LeCroy.com

## Abstract

Signal Integrity engineers are typically simulating systems using simulation models and measuring signals in systems using instruments. Often, during the design process, simulated models are replaced with measurement based models – those typically generated using a VNA or TDR. There is often confusion during this process for two reasons. First, the measurement based models often look different than the simulation models. Second, the measurement based models and simulation based models produce different waveform results in simulation. This is compounded by the fact that systems nowadays are usually differential. Engineers need some insight to validate measurement based models.

This paper provides basic information on how to interpret s-parameter based models and how to create reasonable expectations on the measurement methods and on the models performance. It also provides methods to tie simulation and measurement together to validate models through time-domain co-simulation – the process of mixing real measurements and simulation techniques.

## Author(s) Biography

Pete Pupalais was born in Boston, Massachusetts in 1964 and received the B.S. degree in electrical engineering from Rutgers University, New Brunswick, New Jersey in 1988.

He joined LeCroy Corporation, a manufacturer of high-performance measurement equipment located in Chestnut Ridge, New York in 1995 where he is currently Principal Technologist. He works for the CTO on technology development for high-speed waveform digitizing systems and his interests include digital signal processing, applied mathematics, signal integrity and RF/microwave systems. During his tenure at LeCroy, he has also served as Product Marketing Manager for the high-end oscilloscope product line. Prior to LeCroy he served in the United States Army and has worked as an independent consultant in embedded systems design.

Mr. Pupalais holds twelve patents in the area of measurement instrument design and is a member of Tau Beta Pi, Eta Kappa Nu and the IEEE signal processing, communications, and microwave societies.

# Introduction

Signal integrity engineers spend large amounts of time and effort applying three important domains of knowledge: theory, simulation, and measurement\*. In particular, large amounts of effort are applied triangulating measurements and calculations at the boundaries between these domains, such as matching electromagnetic field theory to expectations in measurement and simulation and matching simulation with measurement results. The successful signal integrity engineer will match all three. In summary, knowing only one domain or all of the domains in isolation is insufficient. Anyone with any experience knows that measurement is not, in general a good idea to test knowledge of theory because in high-frequency design there is as much science in making the measurement as there is in what is being measured. Of course we also know that using a simulator to test or gain insight into theory is a bad idea because simulators make simplifying assumptions which can produce both very good and very bad results unless one is careful<sup>1</sup>. Common wisdom is that one should know what to expect prior to simulating or measuring anything.

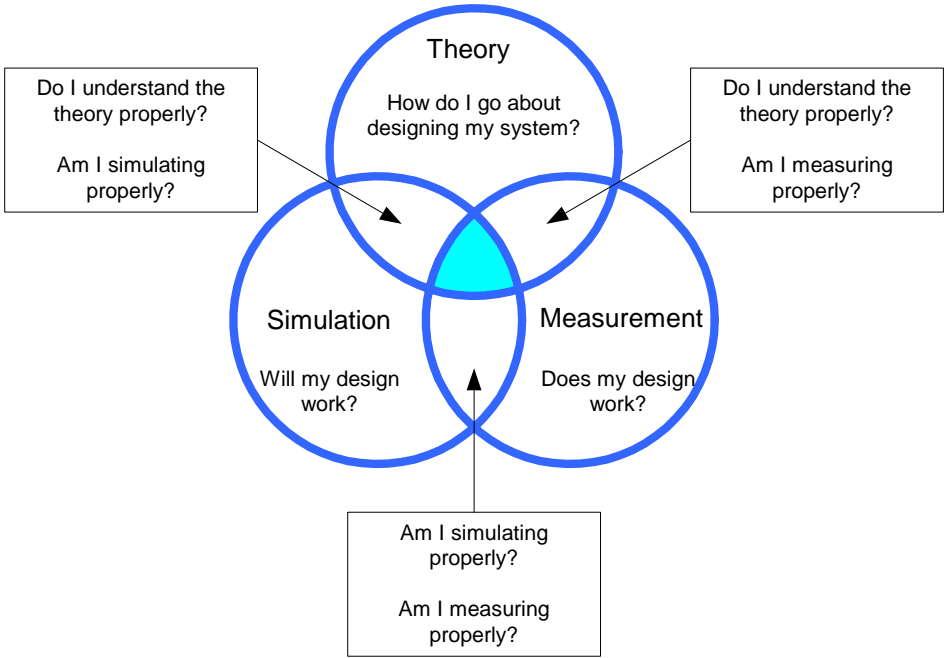


**Figure 1 – The world of the signal integrity engineer**

This paper applies specifically to the matching of theory, simulation and measurement in differential transmission line systems. It approaches the problem in several ways. First, it generally assumes the microwave engineer’s view of the theory of transmission lines – specifically the single-ended transmission line. From this theory, the differential transmission line is developed and simple models are generated. These simple models provide the basis for understanding measurement results. Then, using measurement results of a real differential transmission line, the results are reconciled with the theory using mixed-mode parameters and the impedance profile. The impedance profile is used to convert the measurements of the real

\* This concept was first presented to me by Terry Morris, HP fellow of Hewlett-Packard at a DesignCon planning meeting and formed a method for organizing my thoughts on how to present this topic.

example differential transmission line into a usable model for use in simulation. Then, a concept developed by LeCroy called Virtual Probing™ is used in a co-simulation environment that mixes actual measurements and simulation to verify that the measurement based model is correct. The typical discussion of passivity and causality is not considered in this paper<sup>2 3</sup>.

## Scattering Parameters

Scattering parameters (s-parameters) are parameters that completely determine the behavior of linear networks. Linear networks analysis has been used for a long time using parameters with various forms. These include ABCD, z-, a-,b- and h-parameters, all of which are variations formed from terminal equations involving voltage and current<sup>4</sup>. In the microwave world, s- and t-parameters are most commonly used using terminal equations involving incident and reflected power waves. As speeds increase, the use of s-parameters has been more increasingly used in signal integrity engineering.

The use of power waves (i.e. s-parameters) have certain advantages over the use of voltages and currents in situations where propagation times must be considered. Voltages and currents are more useful in lumped-element circuit analysis where signals are considered to propagate instantaneously. Both methods arrive at the same answers, but the microwave system equivalent models expressed with lumped elements will involve more computational intensity or will have some amount of error when this computational intensity is avoided through simplification of lumped element models. In general, the power wave view is the domain of the microwave engineer.

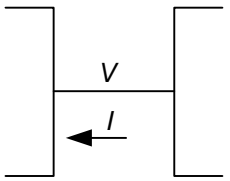
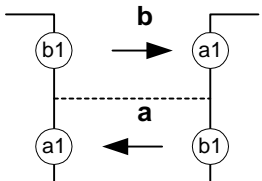
Voltage and Current View	Power Wave View <sup>5</sup>
	
$V = (a + b) \cdot \sqrt{Z_0}$	$a = \frac{V + I \cdot Z_0}{2 \cdot \sqrt{Z_0}}$
$I = (a - b) \cdot \frac{\sqrt{Z_0}}{Z_0}$	$b = \frac{V - I \cdot Z_0}{2 \cdot \sqrt{Z_0}}$

Figure 2 –Voltage/current vs. power waves

## Lumped Element Models

The ideal, lossless, single-ended transmission line is considered as a line whereby along the line there exists a uniformly distributed inductance on the conductor and a uniformly distributed capacitance to ground. This is the circuits view. Transmission lines are not easily modeled accurately with lumped elements.

The characteristic impedance and propagation delay is a function of the inductance and capacitance of the line.

$$Z = \sqrt{\frac{L}{C}} \quad Td = \sqrt{L \cdot C}$$

**Equation 1**

To provide a lumped element equivalent model, one must use sections. Therefore, the lumped element model can only ever be an approximation. There are some rules of thumb to follow. If one uses ten sections, one gets a reasonably accurate model up to the frequency equal to the reciprocal of the propagation delay. The model completely falls apart at about three times that frequency. For every increase in the number of sections, the frequency the model is valid to increases linearly. Therefore we can say that roughly:

$$\text{sections} = F_{\max} \cdot Td \cdot 10$$

**Equation 2**

This means of course that for long time delays and high frequency, numerous sections are needed.

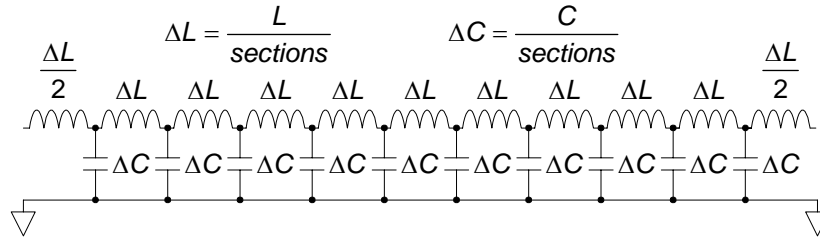


**Figure 3 – Lumped element single-ended transmission line model**

Another view, from an s-parameter viewpoint is a circuit that has a characteristic impedance ( $Z_0$ ) and a propagation delay ( $Td$ ).

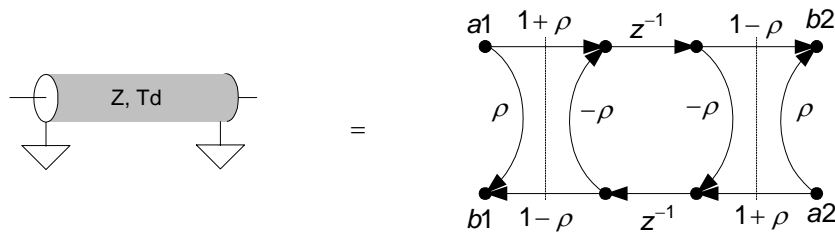


**Figure 4 – S-parameter and signal flow diagram view of the single-ended transmission line**

In order to deal with the s-parameter model shown in Figure 4, one needs to deal with signal flow diagrams<sup>6</sup>. The transmission line shown in Figure 4 has the following s-parameters:

$$S = \frac{\begin{bmatrix} \rho \cdot (1 - z^{-2}) & (1 - \rho^2) \cdot z^{-1} \\ (1 - \rho^2) \cdot z^{-1} & \rho \cdot (1 - z^{-2}) \end{bmatrix}}{1 - z^{-2} \cdot \rho^2}$$

**Equation 3**

where  $\rho = \frac{Z - Z_0}{Z + Z_0}$  and  $z = e^{j \cdot 2 \cdot \pi \cdot f \cdot Td}$  and  $Z_0$  is the reference impedance (usually 50 Ohms) and  $f$  is the frequency.

Examining Equation 3, one can see that when the impedance is matched (i.e.  $Z = Z_0$ ), the s-parameters become:

$$S = \begin{bmatrix} 0 & z^{-1} \\ z^{-1} & 0 \end{bmatrix}$$

**Equation 4**

Equation 4 provides the s-parameters of a perfectly matched, symmetric, lossless transmission line with linear phase. This is an extreme model, but practically, measurements of real single-ended transmission lines are compared to this ideal to provide intuition regarding the behavior of the measured element. In other words, a practical single-ended transmission line will typically reflect a certain amount of the signal at the interface, which is usually small if the line is well matched, and will transmit, with loss, the incident wave from one port to another with delay.

## Differential Transmission Lines

For the differential transmission line case, things become much more complicated. The equivalent lumped-element approximation is shown in Figure 5. Here, there are two single-ended lines, but they are coupled, as indicated by mutual inductance and capacitance. Here we can see that when the lines are uncoupled, they can be viewed as two, independent single-ended lines.

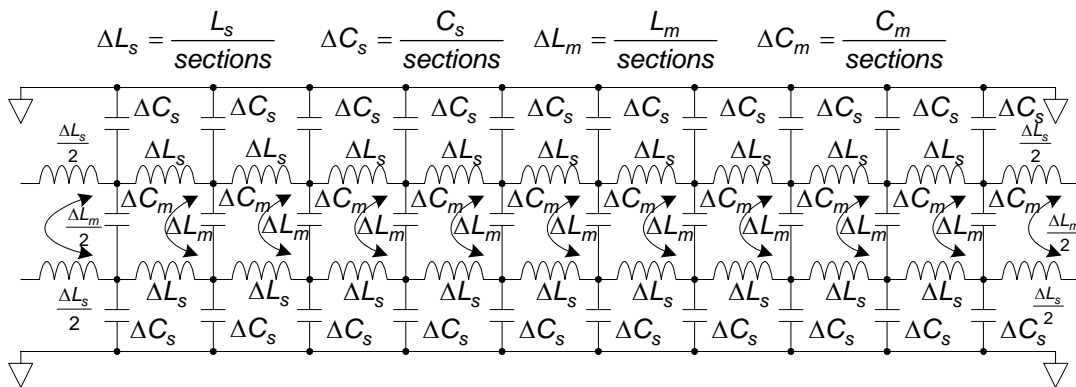


**Figure 5 – Lumped element differential transmission line model**

The equivalent model based on transmission lines<sup>7 8</sup> as shown in Figure 6 is also very complicated. You will note that the model consists of connections of transmission lines with even- and odd-mode impedances and propagation times.

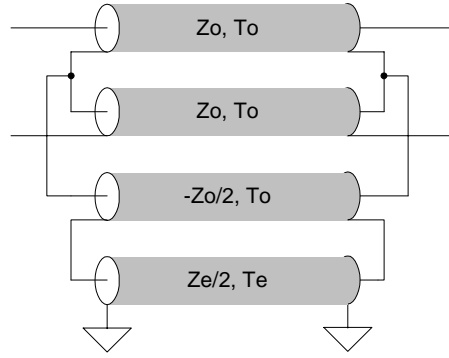


**Figure 6 – Differential Transmission Line Model**

$$Z_o = \sqrt{\frac{L_s - L_m}{C_s + 2 \cdot C_m}}, \quad Z_e = \sqrt{\frac{L_s + L_m}{C_s}}, \quad T_o = \sqrt{(L_s - L_m) \cdot (C_s + 2 \cdot C_m)}, \quad T_e = \sqrt{(L_s + L_m) \cdot C_s}$$

**Equation 5**

A key observation can be made by contrasting the transmission line models for the differential case with the single-ended case. In the case of the single-ended transmission system, we saw that the lumped-element model provides little insight into the behavior of the system. The transmission line model showed that characteristic impedance and time delay provided more insight. In the differential case, one can say that while the model in Figure 6 provides for simplification in computation and some simplification in providing insight, it cannot be considered as a model that provides great amounts insight. This is because the model hides most of the insight into differential behavior.

## The Mode Converter

Mixed mode s-parameters<sup>9</sup> are equivalent to single-ended s-parameters in the sense that they completely define the system behavior; neither being more accurate than the other.

Mixed-mode s-parameters assume that two single-ended ports combine to form a mixed-mode port – one port considered as differential- and the other as common-mode. In other words, consider two single-ended ports with one port labeled “p” and the other port labeled “m”. Port p is assumed to carry the plus portion of a differential signal and port m is assumed to carry the minus portion. The differential and common mode components of a signal applied to ports p and m are defined as\* :

$$V_d = \frac{V_p - V_m}{\sqrt{2}} \quad \text{and} \quad V_c = \frac{V_p + V_m}{\sqrt{2}}$$

**Equation 6**

\* Note that usually, the differential signal is assumed to be the difference between the plus and minus terminals and the common-mode signal is assumed to be the average. The convention in microwave systems is to use a  $\sqrt{2}$  in the denominator of both.

Which means that:

$$V_p = \frac{V_c + V_d}{\sqrt{2}} \text{ and } V_m = \frac{V_c - V_d}{\sqrt{2}}$$

**Equation 7**

Equation 6 and Equation 7 lead to a device shown in Figure 7. This device is very important for differential systems because it is actually the only piece of information you need to know for dealing with mixed-mode systems. All mixed-mode to single-ended s-parameter calculations can be made by simply cascading blocks with the mode converter device.

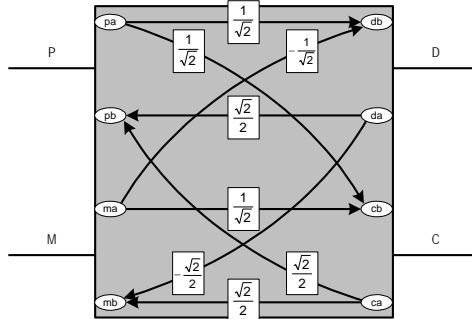


**Figure 7 - Single-ended to mixed-mode converter**

A mode converter has s-parameters that can be inserted into any simulation and is defined as follows:

$$\frac{1}{\sqrt{2}} \cdot \begin{bmatrix} 0 & 0 & 1 & 1 \\ 0 & 0 & -1 & 1 \\ 1 & 1 & 0 & 0 \\ -1 & 1 & 0 & 0 \end{bmatrix} \cdot \begin{bmatrix} pa \\ ma \\ da \\ ca \end{bmatrix} = \begin{bmatrix} pb \\ mb \\ db \\ cb \end{bmatrix}$$

**Equation 8 – S-parameters of the mode converter**

If we consider the t-parameters of the mode converter block  $T_{sm}$  and  $T_{ms}$  having ports 1 and 2 as the single-ended signals and ports 3 and 4 as the differential- and common-mode ports, respectively, then we can find the mixed mode t-parameters  $T_{mm}$  from the single-ended t-parameters  $T_{se}$  as:

$$T_{mm} = T_{ms} \cdot T_{se} \cdot T_{sm} \text{ or vice-versa as: } T_{se} = T_{sm} \cdot T_{mm} \cdot T_{ms} \cdot$$

Alternatively, to convert a single-ended four-port network into a mixed-mode network, converters are simply connected appropriately to the ports of the single-ended network, as shown in Figure 8.

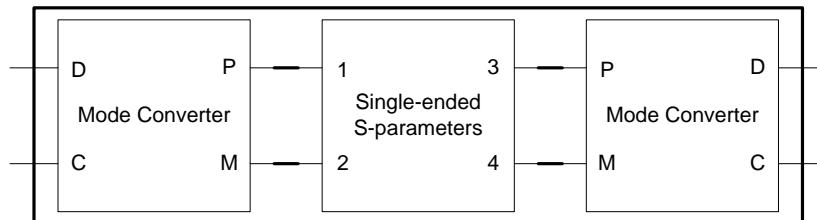


**Figure 8 – Equivalent mixed-mode network**



By manipulating Equation 8, it can be shown that:

$$\begin{bmatrix} sdd_{11} & sdd_{12} & sdc_{11} & sdc_{12} \\ sdd_{21} & sdd_{22} & sdc_{21} & sdc_{22} \\ scd_{11} & scd_{12} & scc_{11} & scc_{12} \\ scd_{21} & scd_{22} & scc_{21} & scc_{22} \end{bmatrix} = \left( \frac{1}{\sqrt{2}} \cdot \begin{bmatrix} 1 & -1 & 0 & 0 \\ 0 & 0 & 1 & -1 \\ 1 & 1 & 0 & 0 \\ 0 & 0 & 1 & 1 \end{bmatrix} \right) \cdot \begin{bmatrix} s_{11} & s_{12} & s_{13} & s_{14} \\ s_{21} & s_{22} & s_{23} & s_{24} \\ s_{31} & s_{32} & s_{33} & s_{34} \\ s_{41} & s_{42} & s_{43} & s_{44} \end{bmatrix} \cdot \left( \frac{1}{\sqrt{2}} \cdot \begin{bmatrix} 1 & -1 & 0 & 0 \\ 0 & 0 & 1 & -1 \\ 1 & 1 & 0 & 0 \\ 0 & 0 & 1 & 1 \end{bmatrix} \right)^{-1}$$

Equation 9

Or<sup>10</sup>:

$$\begin{bmatrix} sdd_{11} & sdd_{12} & sdc_{11} & sdc_{12} \\ sdd_{21} & sdd_{22} & sdc_{21} & sdc_{22} \\ scd_{11} & scd_{12} & scc_{11} & scc_{12} \\ scd_{21} & scd_{22} & scc_{21} & scc_{22} \end{bmatrix} = \frac{\begin{bmatrix} s_{11} - s_{21} - s_{12} + s_{22} & s_{13} - s_{23} - s_{14} + s_{24} & s_{11} - s_{21} + s_{12} - s_{22} & s_{13} - s_{23} + s_{14} - s_{24} \\ s_{31} - s_{41} - s_{32} + s_{42} & s_{33} - s_{43} - s_{34} + s_{44} & s_{31} - s_{41} + s_{32} - s_{42} & s_{33} - s_{43} + s_{34} - s_{44} \\ s_{11} + s_{21} - s_{12} - s_{22} & s_{13} + s_{23} - s_{14} - s_{24} & s_{11} + s_{21} + s_{12} + s_{22} & s_{13} + s_{23} + s_{14} + s_{24} \\ s_{31} + s_{41} - s_{32} - s_{42} & s_{33} + s_{43} - s_{34} - s_{44} & s_{31} + s_{41} + s_{32} + s_{42} & s_{33} + s_{43} + s_{34} + s_{44} \end{bmatrix}}{2}$$

Equation 10

Similarly:

$$\begin{bmatrix} s_{11} & s_{12} & s_{13} & s_{14} \\ s_{21} & s_{22} & s_{23} & s_{24} \\ s_{31} & s_{32} & s_{33} & s_{34} \\ s_{41} & s_{42} & s_{43} & s_{44} \end{bmatrix} = \left( \frac{1}{\sqrt{2}} \cdot \begin{bmatrix} 1 & -1 & 0 & 0 \\ 0 & 0 & 1 & -1 \\ 1 & 1 & 0 & 0 \\ 0 & 0 & 1 & 1 \end{bmatrix} \right)^{-1} \cdot \begin{bmatrix} sdd_{11} & sdd_{12} & sdc_{11} & sdc_{12} \\ sdd_{21} & sdd_{22} & sdc_{21} & sdc_{22} \\ scd_{11} & scd_{12} & scc_{11} & scc_{12} \\ scd_{21} & scd_{22} & scc_{21} & scc_{22} \end{bmatrix} \cdot \left( \frac{1}{\sqrt{2}} \cdot \begin{bmatrix} 1 & -1 & 0 & 0 \\ 0 & 0 & 1 & -1 \\ 1 & 1 & 0 & 0 \\ 0 & 0 & 1 & 1 \end{bmatrix} \right)$$

Equation 11

Or:

$$\begin{bmatrix} s_{11} & s_{12} & s_{13} & s_{14} \\ s_{21} & s_{22} & s_{23} & s_{24} \\ s_{31} & s_{32} & s_{33} & s_{34} \\ s_{41} & s_{42} & s_{43} & s_{44} \end{bmatrix} = \frac{\begin{bmatrix} sdd_{11} + sdd_{12} + sdc_{11} + sdc_{12} & -sdd_{11} - sdd_{12} + sdc_{11} + sdc_{12} & sdd_{12} + sdd_{12} + sdc_{12} + sdc_{12} & -sdd_{12} - sdd_{12} + sdc_{12} + sdc_{12} \\ -sdd_{11} + sdd_{11} - sdc_{11} + sdc_{11} & sdd_{11} - sdd_{11} - sdc_{11} + sdc_{11} & -sdd_{12} + sdd_{12} - sdc_{12} + sdc_{12} & sdd_{12} - sdd_{12} - sdc_{12} + sdc_{12} \\ sdd_{21} + sdd_{21} + sdc_{21} + sdc_{21} & -sdd_{21} - sdd_{21} + sdc_{21} + sdc_{21} & sdd_{22} + sdd_{22} + sdc_{22} + sdc_{22} & -sdd_{22} - sdd_{22} + sdc_{22} + sdc_{22} \\ -sdd_{21} + sdd_{21} - sdc_{21} + sdc_{21} & sdd_{21} - sdd_{21} - sdc_{21} + sdc_{21} & -sdd_{22} + sdd_{22} - sdc_{22} + sdc_{22} & sdd_{22} - sdd_{22} - sdc_{22} + sdc_{22} \end{bmatrix}}{2}$$

Equation 12

In Figure 8, the periphery of the interconnected converters and the four-port network form a mixed-mode network. Similarly, Figure 9 shows an equivalent four-port network created by interconnecting converters and a mixed-mode network.

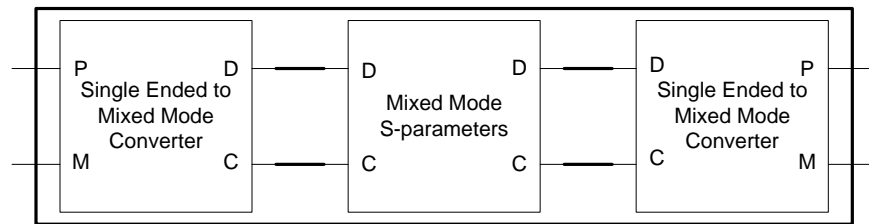
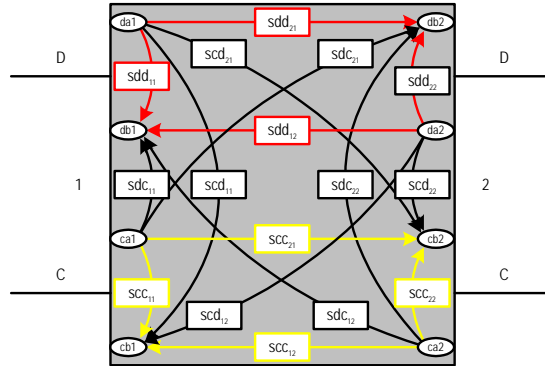


Figure 9 – Equivalent single-ended four-port network

## Typical Differential Backplanes

The mixed-mode s-parameters of a differential device are shown in Figure 10. In Figure 10 all of the mixed-mode s-parameters are shown, but the major terms have been colored. In red, the

differential-mode is highlighted, which is not only of the most interest, but also contains the terms that most affect the behavior of a differential system. In yellow, the common-mode terms are highlighted. The common-mode contains the next most dominant terms which are required for accuracy in simulation when the signals are unbalanced and when single-ended signals are desired.



**Figure 10 – Mixed-mode network**

The remaining terms are the mode-conversion terms. These are usually very small, but are sometimes the terms of interest. If these terms are truly very small, they can be neglected and a reasonable model of an ideal, lossless, differential transmission line shown in Figure 11 can be used.

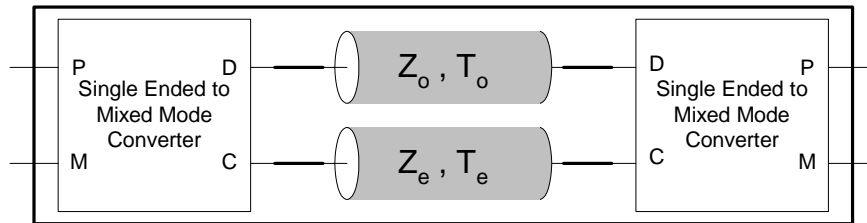


**Figure 11 – Differential backplane**

It is important to point out that the model in Figure 11 has identical behavior as the model in Figure 6, but unlike Figure 6, Figure 11 exposes a lot of insight.

The s-parameters of the inner part of the device shown in Figure 11 are provided in Equation 13, which should be contrasted with Equation 3.\*

\* The inner part is the four-port mixed mode device formed by the parallel transmission lines. Remember that Equation 11 are the mixed mode s-parameters, while Equation 3 are single-ended s-parameters. To convert these s-parameters to single-ended, you must use Equation 11 or Equation 12.

$$S = \begin{bmatrix} \frac{\rho_o \cdot (1 - z_o^{-2})}{1 - z_o^{-2} \cdot \rho_o^2} & \frac{(1 - \rho_o^2) \cdot z_o^{-1}}{1 - z_o^{-2} \cdot \rho_o^2} & 0 & 0 \\ \frac{(1 - \rho_o^2) \cdot z_o^{-1}}{1 - z_o^{-2} \cdot \rho_o^2} & \frac{\rho_o \cdot (1 - z_o^{-2})}{1 - z_o^{-2} \cdot \rho_o^2} & 0 & 0 \\ 0 & 0 & \frac{\rho_e \cdot (1 - z_e^{-2})}{1 - z_e^{-2} \cdot \rho_e^2} & \frac{(1 - \rho_e^2) \cdot z_e^{-1}}{1 - z_e^{-2} \cdot \rho_e^2} \\ 0 & 0 & \frac{(1 - \rho_e^2) \cdot z_e^{-1}}{1 - z_e^{-2} \cdot \rho_e^2} & \frac{\rho_e \cdot (1 - z_e^{-2})}{1 - z_e^{-2} \cdot \rho_e^2} \end{bmatrix}$$

Equation 13

where  $\rho_o = \frac{Z_o - Z_0}{Z_o + Z_0}$  and  $z_o = e^{j \cdot 2 \cdot \pi \cdot f \cdot T_o}$ ,  $\rho_e = \frac{Z_e - Z_0}{Z_e + Z_0}$  and  $z_e = e^{j \cdot 2 \cdot \pi \cdot f \cdot T_e}$  and  $Z_0$  is the reference impedance (usually 50 Ohms) and  $f$  is the frequency.

Examining Equation 3, you can see that when the impedance is matched (i.e.  $Z_e = Z_o = Z_0$ ), the mixed-mode s-parameters become:

$$S_{mm} = \begin{bmatrix} 0 & z^{-1} & 0 & 0 \\ z^{-1} & 0 & 0 & 0 \\ 0 & 0 & 0 & z^{-1} \\ 0 & 0 & z^{-1} & 0 \end{bmatrix}$$

Equation 14

But, applying Equation 12, we see that this leads to Equation 15:

$$S_{se} = \begin{bmatrix} 0 & 0 & z^{-1} & 0 \\ 0 & 0 & 0 & z^{-1} \\ z^{-1} & 0 & 0 & 0 \\ 0 & z^{-1} & 0 & 0 \end{bmatrix}$$

Equation 15

Equation 15 contains the single-ended, four port s-parameters of a system with two single-ended uncoupled lines. This is shown in Figure 12.

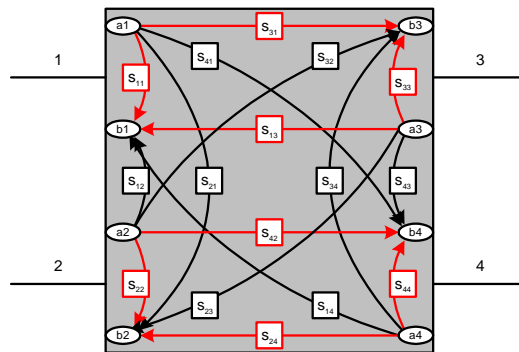


Figure 12 – Single-ended s-parameters of uncoupled differential transmission line

Equation 15 comes from the fact that in order to match the even and odd mode impedances, the lines must be completely uncoupled. This can be seen by examining Equation 5, where you can see that if a line has non-zero self inductance and self capacitance, then the only way for the even and odd mode impedances of two lines used for differential transmission to be equal is for the mutual capacitance and mutual inductance to be zero. By the way, equivalence of the even- and odd-mode impedance also dictates that the even- and odd-mode propagation time is also equal, also seen in Equation 5, hence the use of a single  $z$  in Equation 14.

Therefore, we can see that the case of the uncoupled line is an uninteresting case that does not require any special insight offered through mixed-mode analysis. It is useful to test whether this situation is indeed the case for a differential system. This case can be determined by simply comparing the single-ended s-parameters of single line of a differential pair measured with the other line terminated in an open, short, and load. If the measured two port s-parameters are unchanged, then you know that the lines are in fact de-coupled and analysis proceeds using single-ended analysis techniques.

In practice, however, the lines are coupled to some extent – usually to an extent worthy of considering in a model. The design goal in this case is usually to have the odd-mode impedance matched to 50 Ohms. This means that the even-mode impedance will be greater than 50 Ohms (the even-mode impedance is always higher than the odd-mode impedance in a coupled line) and the even- and odd-mode propagation times will be different.

## Measurements of Differential Transmission Lines

Differential transmission line characteristics are measured using either a vector-network-analyzer (VNA) or time-domain reflectometry (TDR). Both of these instruments have various strengths and weaknesses relative to each other that have been argued ad nauseam, but it is worthwhile to point out that generally, the VNA measures single-ended s-parameters and software is utilized to convert to mixed-mode s-parameters. A TDR can measure either single-ended s-parameters or mixed mode s-parameters directly by stimulating the differential system with odd-mode and even-mode steps. Either way the same theory applies for calibration and measurement<sup>11 12</sup>. For the remainder of this paper, only mixed-mode measurements of the transmission line will be considered, whether measured directly or through conversion of single-ended measurements.

Regardless of how the differential transmission line characteristics are measured, a typical measurement problem, as we shall see, is fixturing. Fixturing is the method by which the measurement instrument is connected to a device-under-test (DUT). In many cases, fixturing is both unavoidable and causes significant measurement error. It is unavoidable in cases where the measurement instrument reference plane connectors do not match the connectors on the DUT. It causes significant measurement error when the characteristics of the fixturing is non-ideal as often occurs in high-frequency measurements.

## An Actual Transmission Line Measurement Example

Our analysis utilizes a transmission line as shown in Figure 13. Here we have a 24 inch line running in a serpentine pattern on a board. The line is microstrip on a substrate of glass-epoxy (FR-4) material with a buried ground plane under the traces.

Using a VNA and TDR, s-parameters are measured for this board. Since we already know that single-ended s-parameters are not very interesting, Equation 10 is used to convert the measured s-parameters to mixed-mode. The magnitude is plotted in Figure 14.

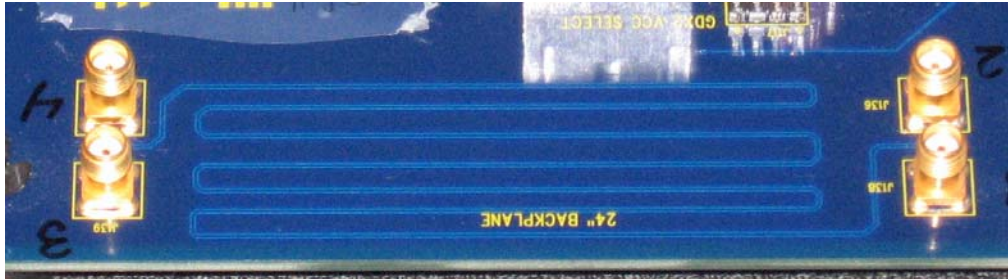


Figure 13 – Differential backplane used for analysis

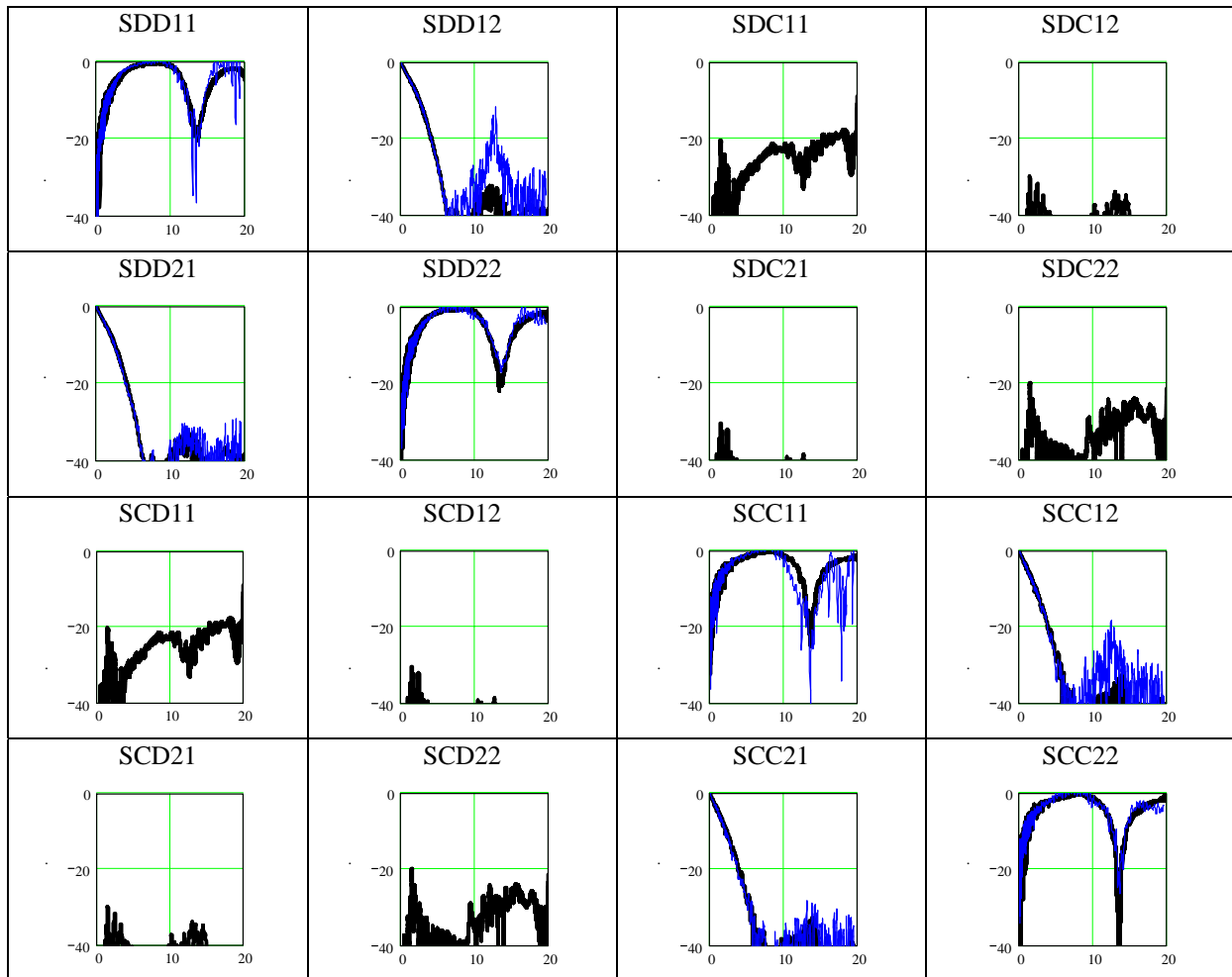
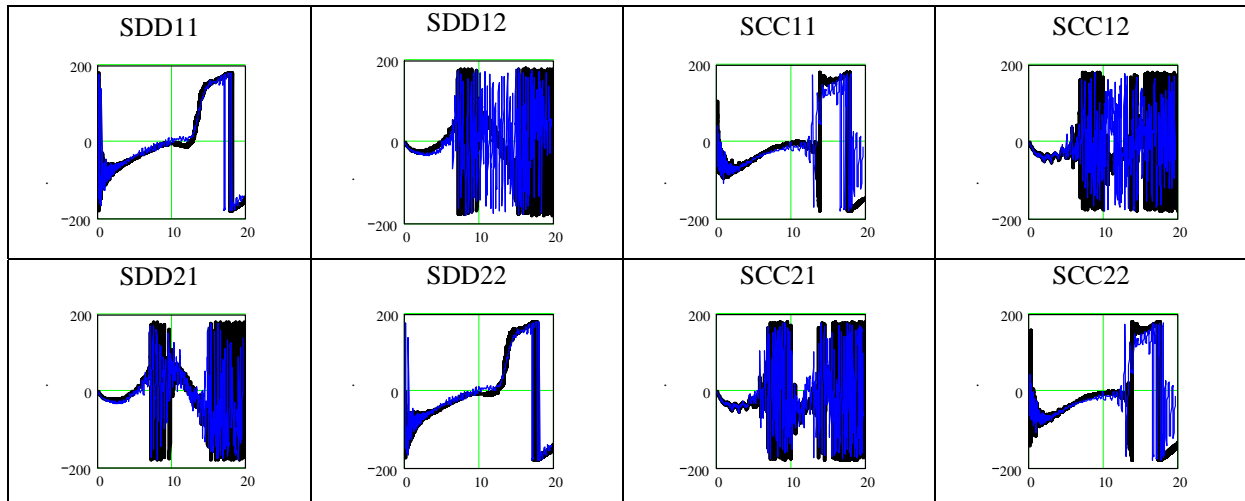


Figure 14 – Mixed-mode s-parameters (magnitude) of differential backplane (blue is TDR, black is VNA)



**Figure 15 - Mixed-mode s-parameters (phase) of differential backplane (mode conversion terms omitted) (blue is VNA, black is TDR)**

Based on what one would expect, here is some commentary on these measurements:

1. The mode-conversion terms (SCD and SDC) are very small (virtually negligible) meaning that each of the two traces in the differential line are similar, as expected.
2. The differential mode terms (SDD) and the common mode terms (SCC) are similar in magnitude, as expected.
3. The terms are the same when viewed from each port, meaning the line is symmetric (i.e.  $SDD12 \approx SDD21$ ,  $SDD11 \approx SDD22$  etc.), as expected.
4. There is loss in the through response terms, as expected.
5. The return loss is poor. This is not expected.
6. The TDR and VNA measurements differ slightly – it is yet unknown whether the differences are important.

One might expect to see poor return loss if the differential or common mode impedances were not close to 50 Ohms, but for a lossless line of this length, there would be a lot of ripple with frequency. Since the line is very lossy, we would expect essentially a line at some dB value based on the characteristic odd- or even-mode impedance. Instead, we see an odd shape with a very long ripple (meaning it is due to some relatively short element). We will look more into this later.

The phase is plotted in Figure 15. Normally the phase is a mess to look at. As an opponent of typical phase unwrapping algorithms, the s-parameters are multiplied by a complex exponential of the form  $e^{j2\pi f \cdot Td}$ , where  $Td$  is the expected propagation time value until the phase is roughly flat. The phase is of no concern when the magnitude is small. In the case of these plots, the time delays used are 3.7 ns for the differential mode through response, 3.9 ns for the common-mode through response and .13 ns for the return response. The different propagation times for each mode shows that the lines are indeed coupled; that the even mode impedance is higher than the odd-mode impedance; and that the propagation velocity is roughly 1.9 ns/foot. The fact that the return response shows a 130 ps propagation time is very suspicious.

A model of the line is constructed in Genesys\* as shown in Figure 16. This is a practical example of matching simulation to measurement – in this case using a model (as opposed to an electro-magnetic simulator). The model is constructed using a substrate matching the board material with estimates of the trace geometries that match the transmission line construction. The key mixed-mode s-parameters are shown in Figure 17. This model shows a rippled return loss that at higher frequencies matches the characteristic impedance of the line for each mode. Again, the match at higher frequencies is due to the losses. The odd-mode return loss is approximately -34 dB, which corresponds to an odd-mode impedance of 48 Ohms. The even-mode return loss is approximately -17 dB which corresponds to an even-mode impedance of 65 Ohms. The return loss characteristic does not match the measured response.

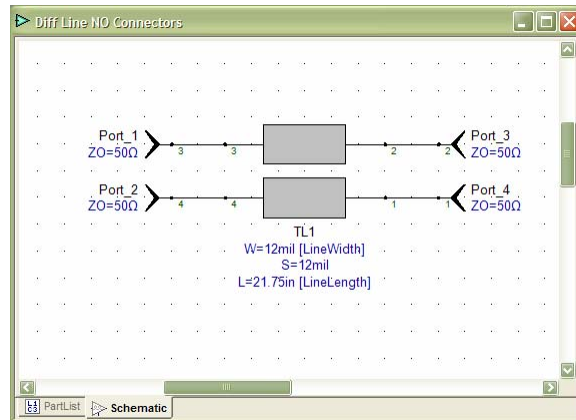


Figure 16 – Genesys transmission line model

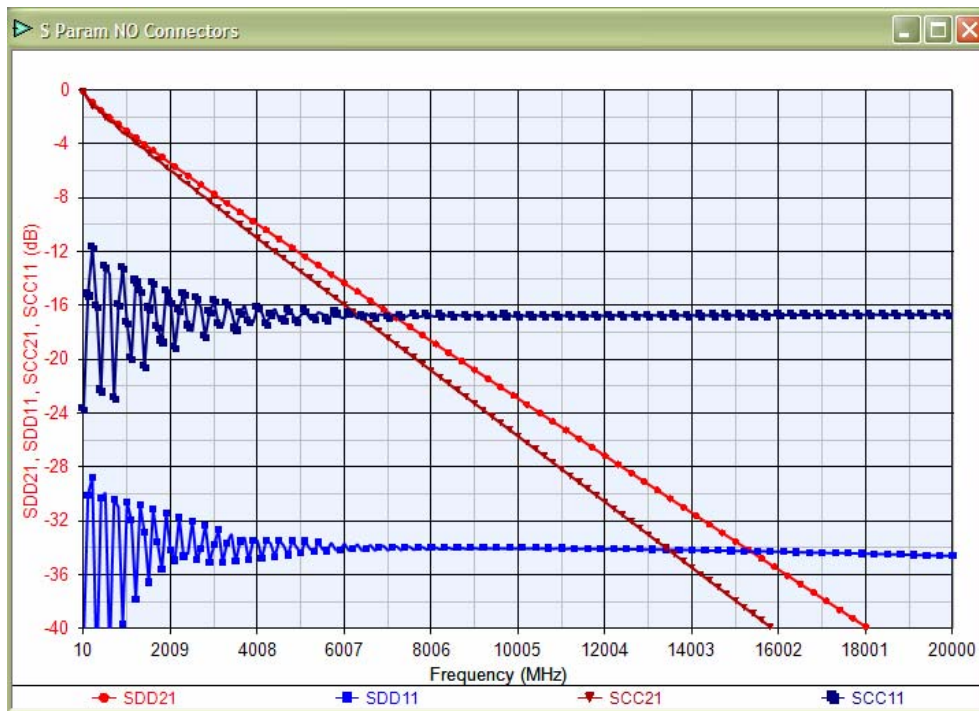
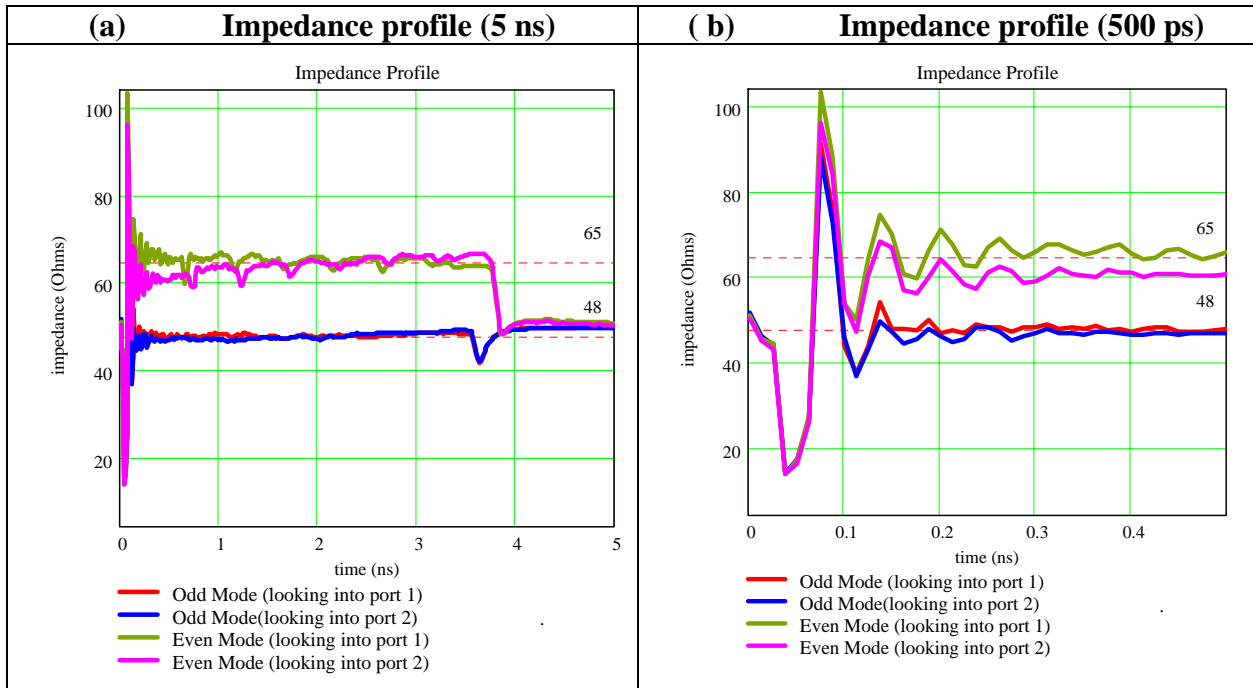


Figure 17 – Expected mixed-mode s-parameters

\* Genesys is a tool provided by Eagleware, now part of Agilent

## Impedance Profile of Example Transmission Line

Returning to our example, the impedance profile of the example transmission line is calculated using SDD11, SCC11, SDD22, and SCC22. The latter two are utilized to look at the impedance profile backwards from port 2. The impedance profile is shown in Figure 18.



**Figure 18 – Impedance profile calculated for example transmission line**

In interpreting Figure 18a, one comes to the following conclusions:

- The odd-mode impedance of the transmission line is 48 Ohms, as expected.
- The even-mode impedance of the transmission line is 65 Ohms, as expected.
- All impedances reach 50 Ohms once the far-end is reached, as expected.
- The odd-mode propagation time is 3.7 ns, as expected.
- The even-mode propagation time 3.9 ns, as expected.
- There is a large impedance discontinuity early in time (other than the step discontinuity to reach the line impedance).
- There is a smaller, wider discontinuity that looks purely capacitive at the end of the line.

Regarding the last observation, we should conclude that our view of the opposite end of the line is less accurate due to the loss in the line (we have assumed no loss in our impedance profile calculation), and therefore the reflected energy becomes smaller due to loss and dispersion along the line. Furthermore, Figure 18 shows the impedance profile taken looking into each port. Assuming that the connector is small and lossless, the characterization of connector interface early in time looking into a port should be fairly accurate. The impedance profile for the first 500 ps of the line is shown in Figure 18b.

Examining Figure 18b, one can understand now the 130 ps value used to straighten out the phase of the return measurements in Figure 15. The connector itself is about 130 ps in length and is not



ideal. A look at the bottom of our differential backplane board shown in Figure 19 sheds some light on why the connector is important to consider in this case. One can see that the center conductor from the SMA connectors are soldered to a via and that the center pin extends through the back of the board. A more accurate measurement would have a better connector or the center conductor drilled back to the via location on the top of the board, but this serves as an example of considerations that must be made when considering fixturing.



Figure 19 – Bottom view of differential backplane board used for analysis

## Impedance Peeled Connector Characteristics

We use a gated version of the impedance profile to calculate the s-parameters of the connectors (using the first 130 ps of the calculation of  $\rho$  for both modes, looking into both ports. Some s-parameters of the connector are plotted in Figure 20. Here are some statements we can make about the connectors:

- They seem to be very similar in characteristics at each port.
- The connectors are the dominant effect of the poor return loss.
- The poor return loss contributes greatly to the loss in through-response.

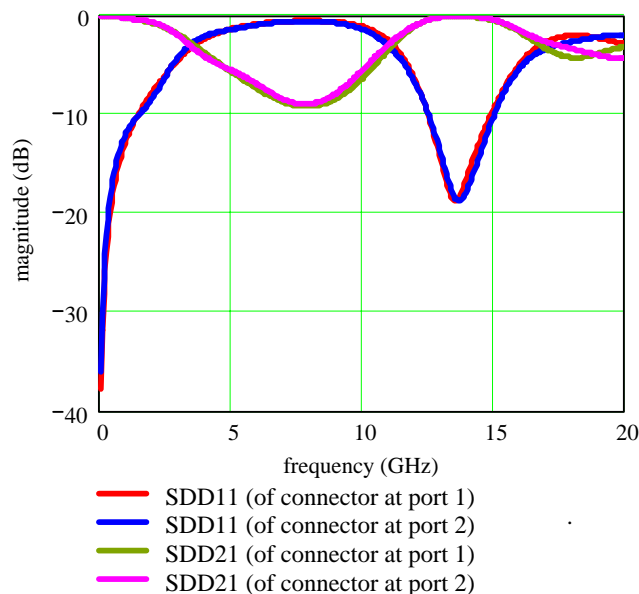


Figure 20 – S-parameters of connector model

# Connector De-embedding

To remove the connectors from the measurement, Equation 16 is used:

$$snc_n = t2s \left( s2t \left( \begin{bmatrix} sc1_{11} & sc1_{12} \\ sc1_{21} & sc1_{22} \end{bmatrix} \right)^{-1} \cdot s2t(s_n) \cdot s2t \left( \begin{bmatrix} sc2_{22} & sc1_{21} \\ sc1_{12} & sc1_{11} \end{bmatrix} \right)^{-1} \right)$$

Equation 16

Where  $snc$  are the s-parameters of the line with the connectors de-embedded,  $sc1$  are the s-parameters of the connector at port 1,  $s$  are the original s-parameters measured for the transmission line, and  $sc2$  are the s-parameters for the connector at port 2 and the function  $s2t(s)$  and  $t2s(t)$  are functions that convert between t- and s-parameters. These functions can be found in common tools for dealing with microwave measurements<sup>13</sup>. It is very important to note the orientation of the connector at port 2. Remember, its s-parameters were calculated looking into port 2, so its port numbers must be reversed in the calculation. Equation 16 is considered for both the differential- and common-mode s-parameters.

Plots of the transmission line with the connectors de-embedded is now shown in Figure 21. The s-parameters with the connectors are shown in blue, and the s-parameters without the connectors is shown in black. Here, one can see that the differential-mode return loss has improved greatly, and the common-mode return loss has reached its expected value of near -17 dB. The big improvement is in the differential through response. It seems that we now have a reasonable measurement based model for the transmission line.

As a check, the newly computed s-parameters and the impedance profile is shown in Figure 21 and Figure 22.

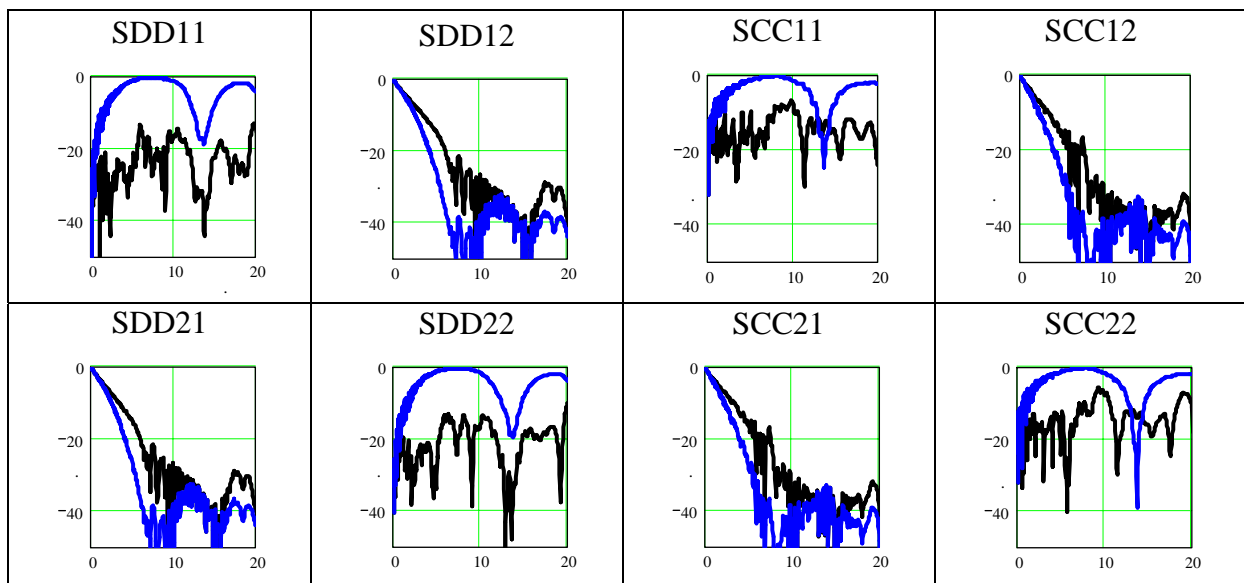


Figure 21 - Mixed-mode s-parameters (magnitude) of differential backplane with connectors de-embedded (blue is before de-embedding and black is after)

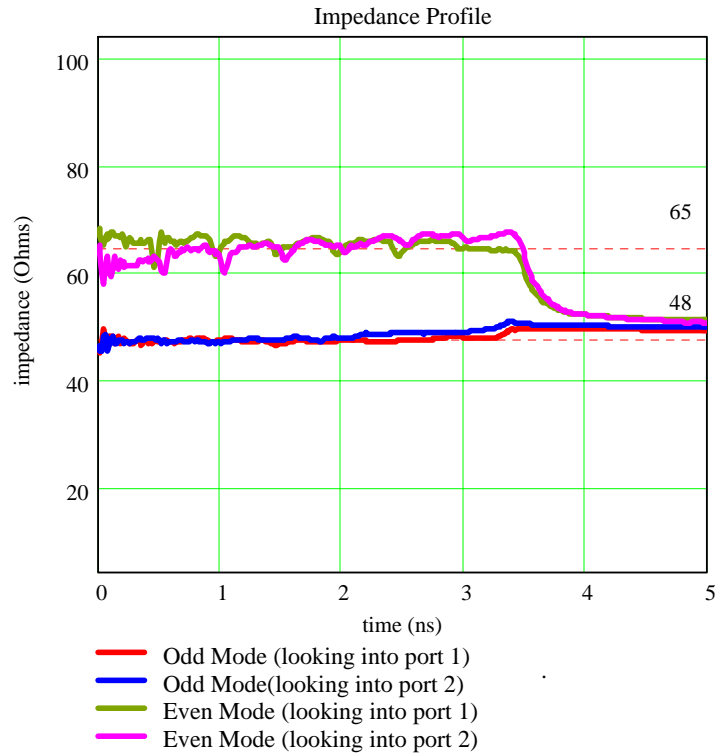


Figure 22 – Impedance profile of transmission line with connectors removed

Considering the board architecture, a new Genesys model of the backplane is generated with the connectors considered as essentially open stubs at the connector. This model generates the s-parameters shown in Figure 24 which match well with those previously measured in Figure 14 and Figure 15.

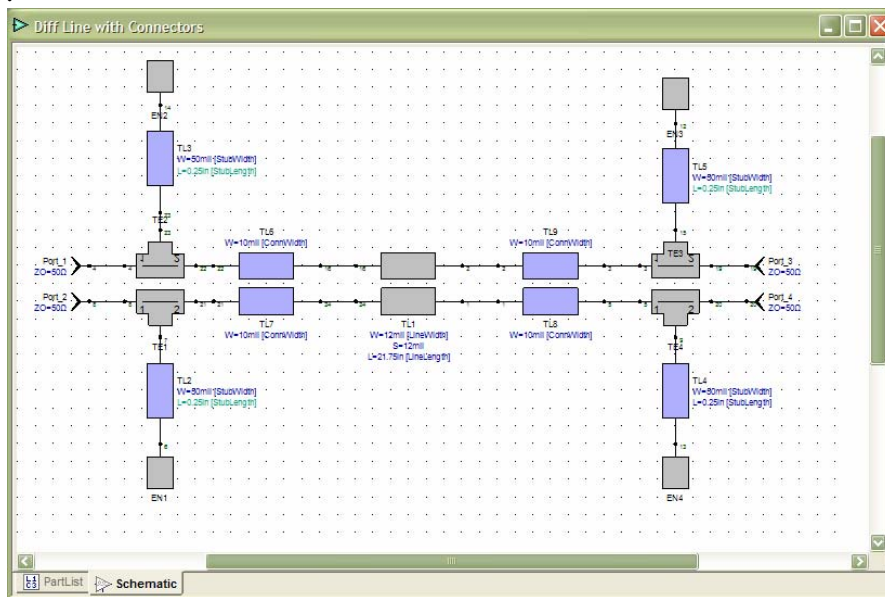


Figure 23 – Genesys model of system with connectors

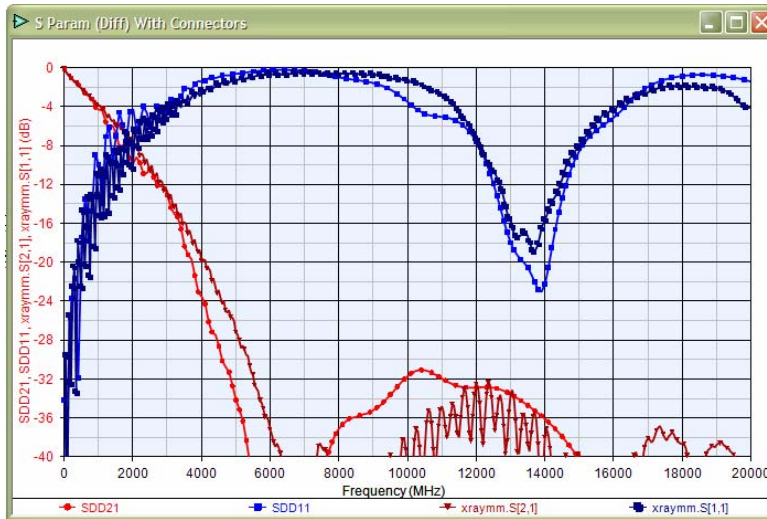


Figure 24 – S-parameters of new model with connectors

## Measurement Based Models

At this stage, it is important to keep in perspective what has been done:

1. Directly measured the backplane using a TDR and VNA.
2. Generated a model of the expected backplane performance.
3. Reconciled the measurement and model by considering the fixturing by:
  - a. Examining the impedance profile
  - b. De-embedding the connectors
  - c. Building the connectors into our model

At this point, we have a reasonable expectation of the ability of a measurement based model, both with and without the fixturing, to match the performance of the backplane.

The measurement based model characteristics that have been measured / calculated serve two key purposes:

- 1) They provide measurable parameters or metrics that determine or infer system behavior.
- 2) They provide models for use in simulation.

In the first case, a compliance standard might specify the loss of a transmission line over certain frequencies or its impedance match. In the construction of a system, these parameters are measured and validated against stated criteria. In the second case, the model will be used in design simulations to determine other design performance. Specifically, one would like to see what the eye-diagram might look like at the receiver when data is transmitted over the differential line.

The remainder of this paper assumes the latter use, but it is important to note that the techniques that will be shown are useful in further validating the measurement based model. In short, even if the goal was to simply measure the line characteristics, the subsequent methods are useful in ensuring that the measurements were made properly. The reason why this is so important is that in the example provided we have fixturing that is obstructing the view of the underlying performance. While this fixturing has been de-embedded in a logical manner, it would be good

to have further confidence in the de-embedding procedure. This is obtained through usage of the model in a time-domain environment – specifically in a co-simulation environment where both the model and real time-domain measurements are utilized.

## Time-Domain Co-Simulation and Verification

Virtual probing<sup>14</sup> is a LeCroy developed tool that allows measurements made on a digital oscilloscope and measurement based models to be combined in a manner to observe waveforms in a system.

Figure 25 shows a system description diagram that determines how a virtual probing measurement is to take place. In this example, one sees four parallel paths, from left to right where the signal flows from top to bottom. The first path is the connection of a transmitter to the measurement instrument and determines the measurement configuration. It describes the environment by which the oscilloscope will acquire waveforms from a transmitter. One observes that the return loss characteristics of the scope, transmitter, and cabling is considered through the use of models or measurements of these device characteristics. The next three paths are called output configurations and determine how waveforms to observe will be determined. The first path is for a measurement of what a waveform would look like when transmitted directly by the transmitter through the backplane (with the fixturing removed) and is the actual measurement goal. The second two paths are used to correlate measurement results with reality. Specifically, it shows what the receiver signal should look like if the measurement based model is used in a co-simulation based on direct reception of the transmitter waveform. It uses two models – one derived from direct mixed-mode TDR measurements and the other derived from single-ended VNA measurements. Note that virtual probing recognizes a mode-converter element.

The first step is to perform the correlation. This is performed by first connecting the scope as in the third and fourth path in the system description diagram. The equipment configuration is shown as the first picture in Figure 26. In this configuration, the oscilloscope is utilized to measure the waveform at the end of the backplane when the internal PRBS generator to the oscilloscope is delivered to the backplane. The waveform is acquired and stored in memory.

The second step is to use virtual probing to co-simulate the waveform at the receiver using the measurement based model. The scope is connected as shown in the second picture in Figure 26. Note that in this configuration, the transmitter connected directly to the oscilloscope channel (i.e. the scope receives the waveform directly from the transmitter). This configuration is synonymous with the first path in the system description diagram.

The virtual probing software is then utilized with waveforms acquired in this manner and with a net-list generated from the diagram in Figure 25 to show what waveforms would look like at the output nodes. The scope captures the waveform directly from the transmitter and uses internal calculations to calculate a transfer function that converts the two measured waveforms into the two differential waveforms labeled PDM, MDM, PC and MC in Figure 25. The results of the acquisition and calculation are shown in Figure 27.

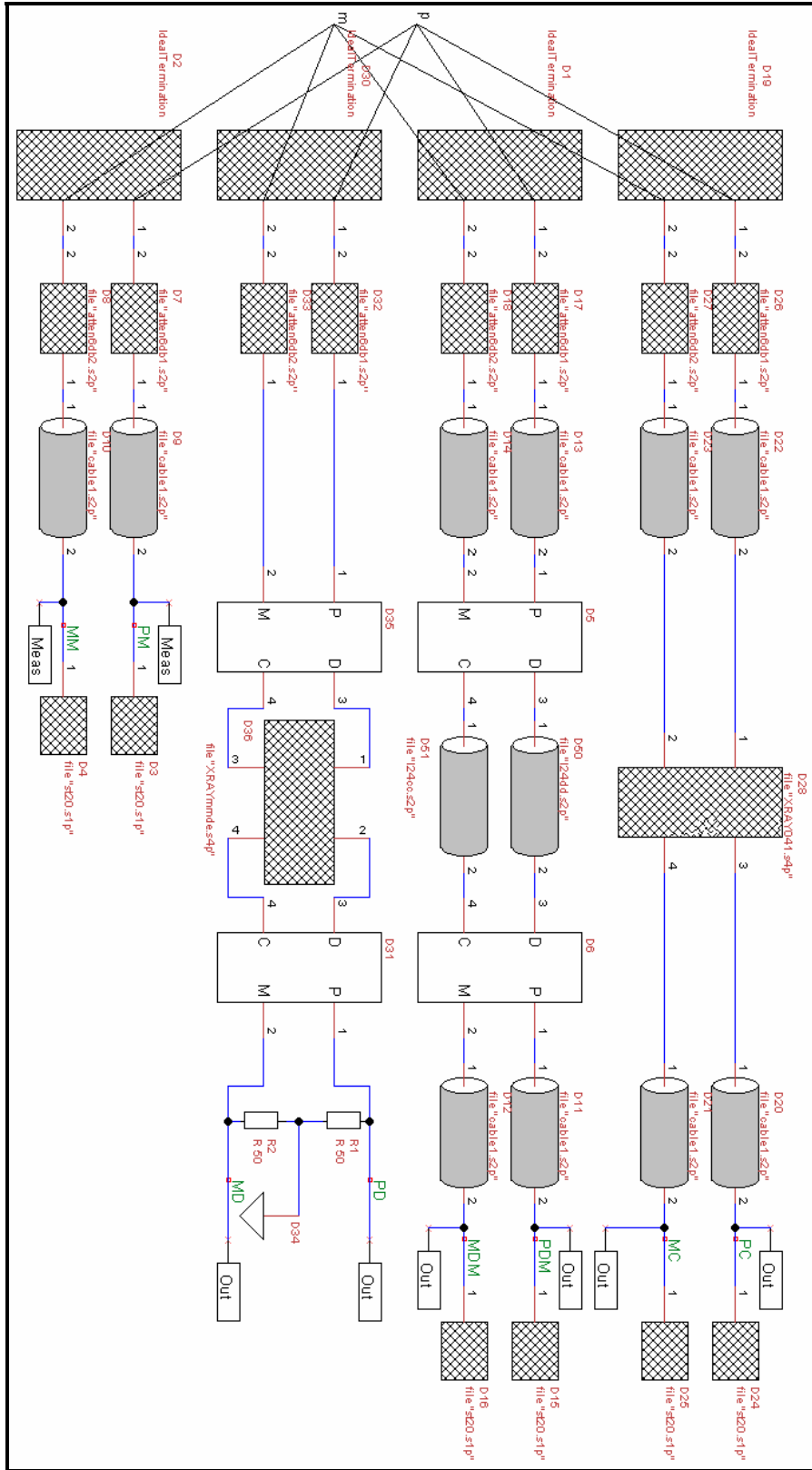
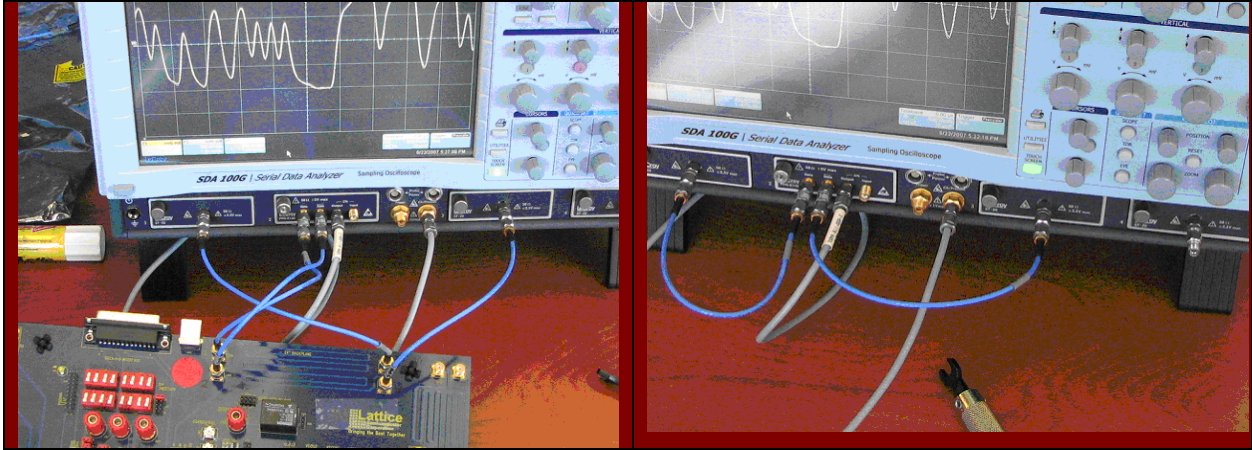


Figure 25 – Virtual probing system description diagram





**Figure 26 – LeCroy WaveExpert in measurement and virtual probing configuration**

In Figure 27, F1 and F2 represent the differential waveforms created by waveform subtraction of the positive and negative waveforms predicted for the VNA and TDR based measurement models. M1 is a memory trace containing the previously stored direct measurement. One can observe that the waveforms lie almost directly on top of each other in both time and voltage. This measurement has several implications:

1. Virtual probing actually works and correctly predicts the time domain waveform at the receiver due to an incident transmitter waveform.
2. The measurement based models of the cabling of the differential backplane are all correct to the extent that they can be safely used in simulation.
3. While not directly compared (direct comparison is impossible) it lends confidence that the measurement based model of the backplane with the fixturing de-embedded is a correct model and is correct for time-domain simulations.

While not the topic of this paper, it also shows that the TDR based model, while lacking in dynamic range compared to the VNA, produces a correct time-domain simulation which after all is the true measure of the measurement based model validity.

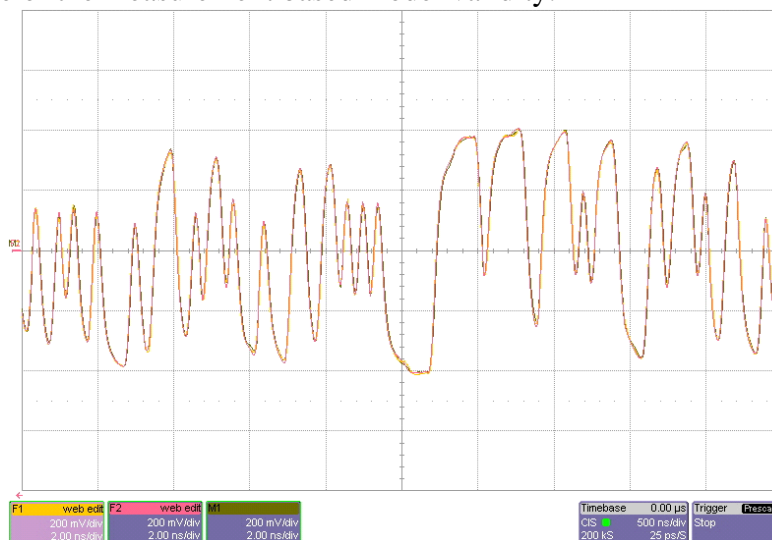


**Figure 27 – Comparison of virtually probed and directly measured waveforms**

## Time-domain Validation

As mentioned previously, the virtual probe generates transfer functions to convert directly measured waveforms into waveforms that would appear at other locations. The various differential and common mode impulse responses calculated are shown in Figure 28.

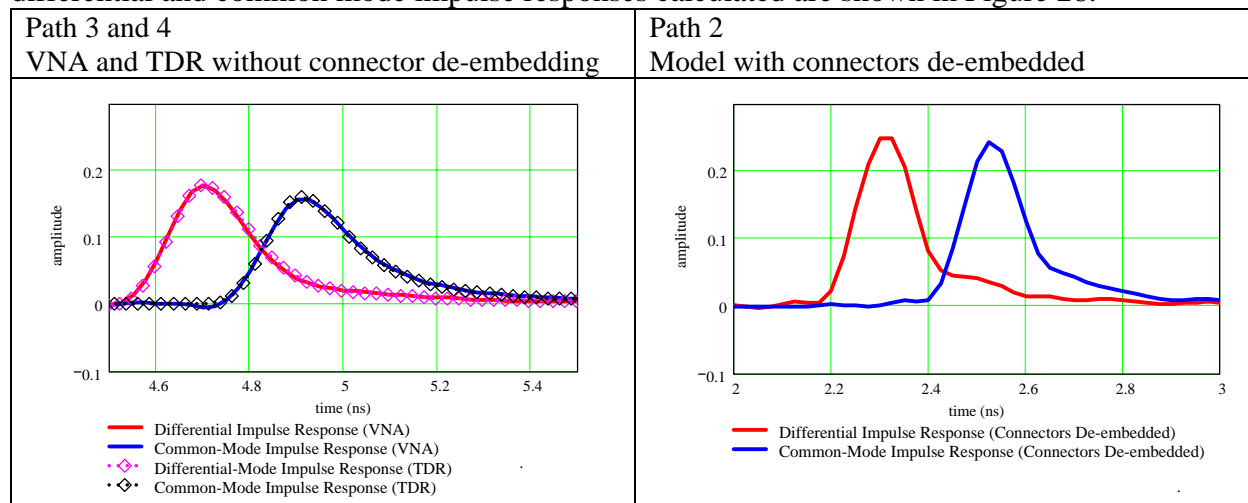


**Figure 28 – Differential- and Common-mode Impulse Responses\***

It shows again that the TDR and VNA responses match. Also, the de-embedded backplane impulse response is better as predicted in Figure 21. One also notes that in both plots, the common mode response is delayed from the differential response by approximately 200 ps, as expected. At first, one might think that there is an error in the timing as the de-embedded impulse occurs at 2.3 and 2.5 ns (remember that the line is 3.7-3.9 ns long), but remember that the connectors have been de-embedded, but most importantly, the impulse response is a transfer function between the measured waveforms at the scope input to the waveforms at the receiver. The scope connection contains about 1 ns of extra cabling and the virtual probe calculation correctly removes this cable in the calculation (see path 1 in Figure 25 to understand this). In other words, time calculated from the impulse response is actually the electrical length of the backplane minus the electrical length of the cable. Note that the impulse responses shown in Figure 28 are valid only when a transmitter signal is connected as in path 1 (the measurement configuration). This is why system co-simulation is so desirable because it considers the entire system in its calculations and uses real waveforms that can be easily correlated like in Figure 27.

Finally, Figure 29 shows the final results using the measurement based model. Here, a simulator is utilized using the model calculated to simulate expectations of compliance to a PCIe gen 2.0 mask and jitter specification. For the simulated transmitter waveform, the backplane is just barely sufficient. As an example of how important it is to tie together the theory, simulation and measurement results, the result of making the calculations on the same transmitter waveform using the backplane without considering the cabling and fixturing. It shows an extra 40 ps of total jitter, mostly due to the ISI created by the connectors!

\* The TDR differential-mode impulse response was adjusted by 20 ps and the common-mode impulse response adjusted by 10 ps to account for minor measurement error to align the impulse responses for shape comparison. This measurement error is considered minor.



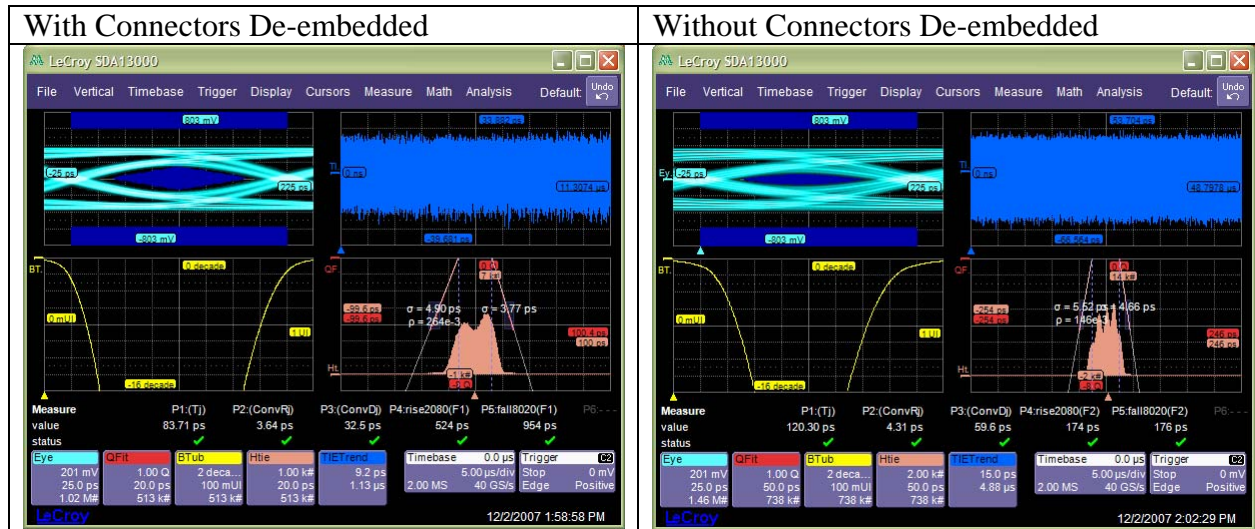


Figure 29 – End goal simulation results using measurement based models

## Summary

This paper outlined steps utilizing an actual differential backplane to make performance measurements. The paper examined circuit theory for differential backplane models to generate proper understanding and expectations of models. It showed mixed-mode frequency-domain measurements and comparisons to theory and utilized fixture de-embedding and to reconcile s-parameter measurements with models. It demonstrated time-domain measurements and co-simulation to directly verify the accuracy of the models generated. Finally, the model was utilized to simulate performance using a 5 Gb/s simulated transmitter waveform.

## References

- <sup>1</sup> B. Pease, *What's all this Spicy stuff, anyhow? (Part IV)*, Electronic Design, Sep 29, 2003
- <sup>2</sup> D. Saraswat, R. Achar, M. Nakhla, "Restoration of passivity in S-parameter data of microwave measurements", IEEE MTT-S International Microwave Symposium Digest, Jun. 2005
- <sup>3</sup> Kaller, D., et al., "Using S-parameters successfully in time domain link simulations", IEEE 14th Topical Meeting on Electrical Performance of Electronic Packaging, Oct. 2005, pp. 95- 98
- <sup>4</sup> James W. Nilsson, "Electric Circuits", Addison-Wesley, 1983
- <sup>5</sup> K. Kurokawa, "Power Waves and the Scattering Matrix," *IEEE Trans. Microwave TheoryTech.*, vol. MTT-13, pp. 194-202, Mar. 1965
- <sup>6</sup> "S-Parameter Design," Hewlett Packard Application Note 154, March, 1990, (5952-1087).
- <sup>7</sup> D. A. Smolyansky and S. D. Corey, "Characterization of differential interconnects from time domain reflectometry measurements," *Microwave Journal*. Vol. 43, no. 3, (2000), pp. 68, 70, 72, 74, 76+
- <sup>8</sup> A. Tripathi, V.K. Tripathi, "A Configuration-Oriented SPICE Model for Multiconductor Transmission Lines in an Inhomogeneous Medium," *IEEE Transactions on Microwave Theory and Techniques*, Vol. 46, No. 12, December 1998
- <sup>9</sup> D. E. Bockelman and W. R. Eisenstadt, "Combined Differential and Common-mode Scattering Parameters: Theory and Simulation," *IEEE Trans. Microwave Theory Tech.*, vol. 43 (Jul. 1995), pp. 1530-1539
- <sup>10</sup> "Three and four port s-parameters: calibrations and mixed mode parameters," Anritsu Application Note, 11410-00279, Nov. 2001
- <sup>11</sup> D. Rytting, "Network Analyzer Error Models and Calibration Methods", presented at Short Course on Computer-Aided RF and Microwave Testing and Design, Rohnert Park, Calif., 1998.
- <sup>12</sup> D. C. DeGroot, J. A. Jargon, K. L. Reed, "Equivalent Circuit Models for Coaxial OSLT Standards", ARFTG Conference, December 2-3, 1999, Atlanta, GA - December 01, 1999.
- <sup>13</sup> "Modeling a Differential High-Speed Backplane in Simulink", [www.mathworks.com](http://www.mathworks.com)
- <sup>14</sup> P. J. Pupalaikis, "Advanced Tools for High Speed Serial Data Measurements", DesignCon 2007, Feb. 2007